A multi-sensor approach to fine-scale fire characterization

I. Csiszar [a,*], T. Loboda [a], N.H.F. French[b], L. Giglio[c], T.L. Hockenberry[b]

[a] University of Maryland, Department of Geography, College Park, MD 20742, USA – icsiszar@hermes.geog.umd.edu
[b] Altarum Institute, P.O. Box 134001, Ann Arbor, MI 48113, USA
[c]SSA/I, NASA Goddard Space Flight Center, Greenbelt, MD 20771, USA

Abstract – Recent improvements in sensor capabilities have enabled fire characterization from satellites. Instantaneous intensities of active fires have been characterized by the Fire Radiative Power (FRP), while burn severity has been assessed from the evaluation of Normalized Burn Ratios (NBR) derived from pre- and post-fire multispectral imagery. MODIS on the Terra and Aqua satellites enables FRP retrievals at a global scale. However, the 1km^2 sub-satellite resolution is too coarse to account for fine scale spatial heterogeneities that are often typical of the burning process. The high resolution (15-90m) ASTER is flown on the Terra satellite, and can be used to determine the location of the active fire front within the MODIS footprint. In this study several fire events in North America were analyzed. MODIS FRP values, localized using ASTER, were combined with burn severity data derived from collocated 30m Landsat TM (Thematic Mapper) and ETM+ (Enhanced Thematic Mapper) imagery for a more complete characterization of the burning process.
Keywords: fires, intensity, severity, satellites.

1. INTRODUCTION

Traditional fire mapping from satellites includes the detection of active fires and burned areas. However, recent improvements in sensor capabilities, the availability of large amounts of high resolution multispectral data and advances in scientific knowledge have also allowed for the characterization of fires. The MODIS (Moderate Resolution Imaging Spectroradiometer) on the experimental polar orbiting Terra and Aqua satellites is the first sensor to enable retrievals of the Fire Radiative Power at a global scale (Justice et al., 2002). FRP is the total integrated instantaneous radiative energy emitted by all fires within the satellite pixel (Wooster et al. 2003):

$$FRP = A_{sa}\,\varepsilon\sigma\sum_{i=1}^{n} f_i T_i^4 \qquad (1)$$

where A = the total area of the satellite pixel [m^2]
ε = fire emissivity
σ = Stephan-Boltzmann constant [5.67x10^{-8} J^{-1}m^{-2}K^{-4}]
f_i = fractional area of the i^{th} thermal component
T_i= temperature of the i^{th} thermal component [K].

For moderate and coarse resolution sensors, such as MODIS, fires typically occupy only a small fraction of the satellite pixel, whereas the entire satellite pixel is represented by a single FRP value. Therefore, it is essential to understand to what extent such moderate resolution observations can be used for fine scale fire characterization.

ASTER (Advanced Spaceborne Thermal Emission and Reflection Radiometer; Yamaguchi et al., 1998) is flown on the same Terra satellite and therefore can provide observations coincident with MODIS. The low saturation of ASTER bands does not allow for the retrieval of FRP at the full range of fire intensities, but it can be used to determine the location of the active fire front within the MODIS pixel. ASTER fire masks have been used to map fire distribution within the MODIS pixel for the evaluation of the binary MODIS fire mask product (Morisette et al., in press). In this study we combined MODIS FRP values with ASTER fire masks to locate fires for finer scale analysis.

Fire characterization based on post-fire imagery – often by comparison with pre-fire data – includes the assessment of burn severity and its within-burn variability. Studies have shown a relationship between reflectance in the near-IR and mid-IR and fuel consumption (Eva and Lambin, 1998, Michalek et al., 2000, Isaev et al., 2002,). The most widespread approach, developed under the joint National Park Service-United States Geologic Survey National Burn Severity Mapping Project, is based on the differencing the Normalized Burn Ratio (NBR) between post- and pre-burn high resolution imagery (Key and Benson, 2004). The methodology has been developed for Landsat Thematic Mapper (TM) or Enhanced Thematic Mapper (ETM+), for which NBR is defined as follows:

$$NBR = \frac{R_4 - R_7}{R_4 + R_7} \qquad (2)$$

where R_4 = band 4 (0.76-0.90 μm) reflectance
R_7 = band 7 (2.08-2.35 μm) reflectance.

The resulting dNBR maps of burn severity are compared to field-based information collected by NPS to determine levels of burn severity for the entire burn. Similarly, FRP has been shown to correlate with instantaneous biomass consumption rate (Wooster, 2002). However, FRP and dNBR are based on observing different stages of the fire process (active burning vs. post-fire effects), using different radiometric signals (emitted thermal radiation vs. reflected solar radiation) and therefore provide the opportunity for more comprehensive fire characterization on a complementary basis. In this study we explored the potential and limitations of such a multi-sensor characterization.

2. DATA

The fire events for this study were selected from a database compiled by the NPS – USGS National Burn Severity Mapping Project. This database contains Landsat imagery, dNBR maps, fire perimeters and metadata for a number of fire sites within National Parks and other federal protected areas. From the database we selected those cases for which ASTER active fire observations were available. ASTER Level-1B Calibrated Radiance at Sensor product files with fire observations were identified by a

* Corresponding author.

coincidence search with MODIS active fire detections, and obtained from NASA's Earth Observing System (EOS) Land Processes Distributed Active Archive Center (LPDAAC).

In addition to the NPS sites we collected data over several independently selected fires and processed them following the NPS procedure (Key and Benson, 2004). For all fires, Landsat TM and ETM+ band data were converted into at sensor reflectances. NBR data were calculated from pre- and post-burn imagery using (2). Then, dNBR maps were derived from geometrically co-registered pre- and post-burn images.

Table A lists the Landsat and ASTER imagery used in this study. The predominant land cover types, as identified by the Boston University 1km MODIS Land Cover Type dataset (Friedl et al., 2002) were Evergreen Needleleaf Forest, Woodland, Grassland and Deciduous Broadleaf Forest. It should be noted that situations when pre- and post-burn high resolution imagery, as well as imagery of the active fires exists are fairly rare and thus the collection of large enough statistically representative sample became a challenging task for this study.

Table A. Summary of Landsat and ASTER imagery

WRS-2 path/row	Preburn date	Postburn date	ASTER date	Number of MODIS fire pixels
38/29	7/15/00	7/5/02	8/28/01	5
72/15	6/23/01	6/17/02	7/9/01	1
34/27	7/6/01	7/9/02	5/13/02	2
24/34	8/14/00	8/28/02	4/5/02	1
66/15	9/12/99	9/8/04	6/21/04	14

3. APPROACH

We used MODIS FRP values from the MOD14 Fires and Thermal Anomalies product (Justice et al., 2002). The MOD14 processing system first executes the MODIS active fire detection algorithm (currently version 4; Giglio et al., 2003) to identify pixels with active burning. FRP values are then derived by the algorithm developed by Kaufman et al. (1998) for pixels flagged as "fire".

For each ASTER image, fire masks were derived using an algorithm developed by Giglio (personal communication). The algorithm generates a binary fire mask at the resolution of the 30m shortwave infrared ASTER bands. The bounding boxes of the coincident MODIS fire pixels were located on each ASTER image. We took into account the fact that the sampling area of each MODIS measurement actually includes the adjacent halves of each neighboring nominal pixel in the scanline. Therefore ASTER fire masks within 2x1 km footprints were used to locate the areas which contributed to the integrated MODIS FRP value.

We also considered the non-homogeneous spatial sampling within the MODIS pixel. In fact, the radiative power recorded by the MODIS sensor is a weighted sum of the instantaneous radiant energy according to the contribution of the area of the pixel to the radiative signal:

$$FRP = A_{sa}\varepsilon\sigma\sum_{i=1}^{n} f_i k_i T_i^4 \quad (3)$$

where k_i = coefficient dependent on the location of the i^{th} thermal component within the pixel.

For MODIS, we used the triangular point spread function (PSF) to normalize the FRP values to a hypothetical rectangular-shaped PSF. The adjusted FRP was calculated as

$$FRP_a = FRP \times n / \sum_{i=1}^{n} k_i \quad (4)$$

where k_i was a simple linear function of the distance of the ASTER pixel from the middle of the MODIS pixel. This formulation also implicitly accounts for a constant f_i (the size of the ASTER pixel) and the assumption of the uniformity of T_i within the ASTER fire mask.

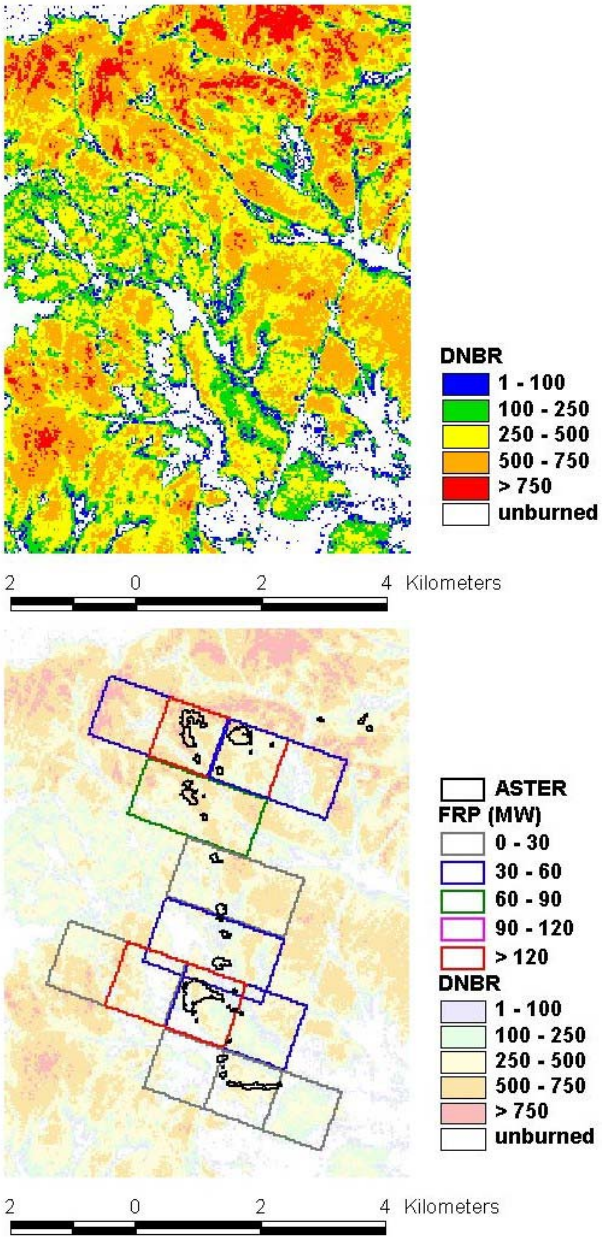

Figure 1. Top: dNBR map of a section of a fire complex in Alaska (WRS-2 path/row 66/15). Bottom: ASTER active fire masks over the same fire complex, with FRP values from MODIS. Active fire data are from 6/21/2004.

ASTER and Landsat imagery were geometrically co-registered with sub-pixel accuracy (RMSE ~ 0.5). The area of the instantaneous active fires as mapped by ASTER was identified on the Landsat-derived dNBR product. Figure 1 shows the dNBR map of a fire complex, the true 2x1 km footprints of the MODIS fire pixels and the location of the ASTER-detected active fires. It can be seen that there is a substantial spatial heterogeneity of burn severity within each MODIS pixel. Also, the same active fires are mapped by two adjacent MODIS observations because of the overlap in the true sampling area on the ground.

4. RESULTS

As it was shown in (1), the single FRP value associated with the ASTER fire mask is a result of the integration of radiative signal from a large number of thermal components. Ideally, the size of the 30m ASTER fire pixel could be considered as the minimum mapping unit of fire components, which could then directly be compared with the dNBR values at the same spatial resolution. However, the ASTER sensor specifications are not optimal for fire characterization and thus the ASTER fire masks could not be resolved further into FRP fields at the ASTER resolution. Comparison of FRP and dNBR was therefore done using summary statistics over the area of the ASTER fire masks only.

Figure 2 shows a comparison of FRP and the mean dNBR over the ASTER fire masks. Although a weak increasing trend can be observed, no significant relationship was found between FRP and the mean dNBR. In particular, there are two outliers with high FRP values of ~ 130 MW. Scrutiny of the data revealed that these observations belong to two large fire complexes with a number of saturated ASTER data. The low saturation of the ASTER bands sensitive to active fires causes artifacts such as spurious saturated data, blooming and spikes around the true fire pixels if the amount of radiation is large (Morisette et al., in press). We found that artifacts in the ASTER data occur when the MODIS FRP exceeds ~ 100 MW. In such conditions there might be some commission errors in the automated ASTER fire mask.

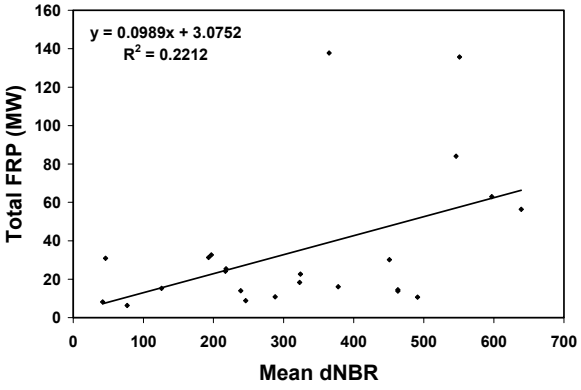

Figure 2. Total Fire Radiative Power against differential Normalized Burn Ratio averaged over the ASTER fire masks.

To ensure that the quality of these data is comparable with the rest used in this study, we visually evaluated ASTER measurements at lower wavelengths, which are normally not used in the fire detection procedure, because of their smaller sensitivity to emitted radiation from fires. Through this procedure we were able to determine that only a small fraction of ASTER pixels represented false detection and concluded that these fires should not be excluded from the analysis.

The relationship between FRP_a and the mean dNBR is shown in Figure 3. It can be seen that the correlation somewhat increased, suggesting that the adjustment of the FRP data makes them more compatible with the uniformly sampled dNBR values. However, the statistical relationship is still weak.

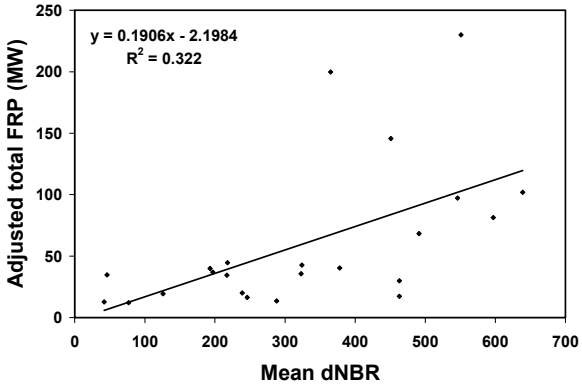

Figure 3. Adjusted total Fire Radiative Power against differential Normalized Burn Ratio and averaged over the ASTER fire masks.

As seen in (1) and (4), the total FRP as measured by MODIS is a combined result of the radiant intensities and fractional burning areas of the various thermal components and the overall extent of burning within the MODIS pixel. Due to the low saturation of ASTER, in this study we could not resolve the radiant intensities at the 30m ASTER resolution. With nearly constant ASTER pixel sizes, however, it was possible to study whether the integrated FRP signal is driven by the variability of radiant intensity or the spatial extent of fires. This is important in order to understand to what extent FRP values at the scale of the MODIS pixel can be used for localized fire characterization.

We normalized FRP data by the area of the ASTER fire mask to make them fully comparable to the mean dNBR values. We found that these quantities are uncorrelated (R^2=0.08 for FRP and R^2=0.26 for FRP_a).

Both this result and the weak relationship between the total FRP and mean dNBR suggest that the FRP measurements are of limited predictive capacity for the burn severity even over the area of the observed active burning within the MODIS pixel. This is also an indicator of the fact that the variability of the integrated FRP values is primarily driven by the number of ASTER fire counts within the MODIS pixel. In fact, there is a strong correlation between the number of ASTER fire pixels and the total FRP (Figure 4).

The fact that FRP, at least in the dataset used in this analysis, is primarily an indicator of the spatial extent of the fire within the MODIS pixel rather than the intensity of the fire, can be explained by the larger natural variability of the number of ASTER fire pixels than the radiant intensity of the fire over a unit area. This is clearly related to the large footprint size of MODIS compared to

the instantaneous burning area. From this one can postulate that for higher spatial resolution sensors such as BIRD (Briess et al., 2003) the FRP signal is increasingly dominated by the radiant intensity.

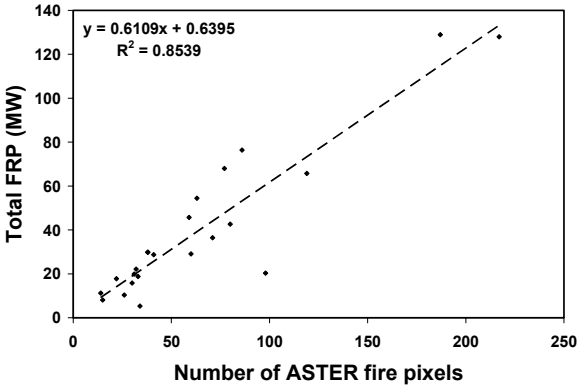

Figure 4. Total Fire Radiative Power against the number of ASTER fire pixels and within MODIS pixels.

5. CONCLUSIONS

Our study has demonstrated that the instantaneous Fire Radiative Power from MODIS is most likely insufficient for the direct evaluation of burn severity. However, FRP is a good indicator of the overall spatial extent of burning and the integrated biomass consumption rate. For full fine scale instantaneous fire characterization higher resolution sensors with proper sensor specifications are necessary. ASTER does not have bands at the optimal spectral region (around ~4 μm) for proper fire detection and characterization. The fire signal in the existing short-wave infrared bands, available only at daytime, are contaminated by reflected solar radiation and saturate for most larger fires even at the lowest sensor gain settings.

The potential for full fire characterization from instantaneous fire observations is also related to the duration and temporal variability of burning. Higher resolution sensors are more likely to collect representative information for faster moving fire fronts. However, even in this case, multiple observations are necessary to observe smoldering, which accounts for a large proportion of mass consumption, emissions and resultant burn severity.

For full evaluation of fire severity and impacts, post-fire assessment is necessary. There has been considerable research in evaluating dNBR for burn severity assessment, including the identification of uncertainties (i.e. van Wagtendonk, 2004). In this study we used the implicit assumption that dNBR is a reasonably accurate measure for burn severity to be used to analyze the information content of the FRP signal. For full evaluation, however, comparison with ground data is necessary.

Results presented in this study were derived from a rather limited dataset due to the lack of pre-burn – active fire – post – burn triplets from high resolution sensors. Our plan is to extend this study, using further data over multiple regions and sensors and to consider variables such as land cover type (fuel type) to determine if the technique may be appropriate for specific fire conditions.

REFERENCES

K. Briess, H. Jahn, E. Lorenz, D. Oertel, W. Skrbek, B. Zhukov, Remote Sensing Potential of the Bi-spectral InfraRed Detection (BIRD) Satellite. *Int. J. Remote Sens.*, vol. 24. pp 865-872, 2003.

H. Eva and E.F. Lambin, Burnt area mapping in Central Africa using ATSR data, *Int.J.Remote Sens.*, vol.19, pp.3473-3497, 1998.

M.A. Friedl, D.K. McIver, J.C.F. Hodges, X.Y. Zhang, D. Muchoney, Global land cover mapping from MODIS: algorithms and early results. *Remote Sens. Environ.*, vol. 83, pp. 287-302, 2002.

L. Giglio, J. Descloitres, C.O. Justice and Y.J. Kaufman, An Enhanced Contextual Fire Detection Algorithm for MODIS, *Remote Sens. Environ.* vol. 87, pp. 273-282, 2003.

A.S. Isaev, G.N. Korovin, S.A. Bartalev, D.V. Ershov, A. Janetos, E.S. Kasischke, H.H. Shugart, N.H.F. French, B.E. Orlick, and T.L. Murphy, Using remote sensing to assess Russian forest fire carbon emissions. *Climatic Change,* vol. 55, pp. 235-249, 2002.

C.O. Justice, L. Giglio, S. Korontzi, J. Owens, J. Morisette, D. Roy, D., J. Descloitres, S. Alleaume, F. Petitcolin, and Y. Kaufman, The MODIS fire products, *Remote Sens. Environ.*, vol. 83, pp. 244-262, 2002.

Y.J. Kaufman, C.O. Justice, L. Flynn, J.D. Kendall, E.M. Prins, L. Giglio, D. Ward, W. Menzel, and A. Setzer, Potential global fire monitoring from EOS-MODIS, *J.Geophys. Res.*, vol. 103, pp. 32215-32238, 1998.

C. Key and N. Benson, Landscape Assessment (LA): Sampling and Analysis Methods, *FIREMON Landscape Assessment V4,* 2004 < http://burnseverity.cr.usgs.gov/methodology.asp>

J.L. Michalek, N.H.F. French, E.S. Kasischke, R.D. Johnson, and J.E. Colwell,. Using Landsat TM data to estimate carbon release from burned biomass in an Alaskan spruce complex. *Int.l J. Remote Sens.,* vol. 21: pp. 323-338, 2000.

J.T. Morisette, L. Giglio, I. Csiszar and C.O. Justice, Validation of the MODIS Active fire product over Southern Africa with ASTER data, *Int. J. Remote Sens.*, special issue for SAFARI2000, in press.

Y. Yamaguchi, A.B. Kahle, H. Tsu, T. Kawakami and M. Pniel, Overview of Advanced Spaceborned Thermal Emission and Reflection Radiometer (ASTER). *IEEE Trans. Geosci.Remote Sens.*, vol. 46, pp. 1062-1071, 1998.

J.W. van Wagtendonk, R.R. Root, C.H. Key, Comparison of AVIRIS and Landsat ETM+ detection capabilities for burn severity, *Remote Sens. Environ.*, vol. 29, pp. 397-408, 2004.

M.J. Wooster, Small-scale experimental testing of fire radiative energy fro quantifying mass combusted in natural vegetation fires, *Geophys. Res. Let.* vol. 29, doi:10.1029/2002GL015487, 2002.

M. J. Wooster, B. Zhukov and D. Oertel, Fire radiative energy for quantitative study of biomass burning: derivation from the BIRD experimental satellite and comparison to MODIS fire products. *Remote Sens. Environ.* 86, pp. 83-107, 2003.